Cancer Cell
Article

Targeting the ANG2/TIE2 Axis Inhibits Tumor Growth and Metastasis by Impairing Angiogenesis and Disabling Rebounds of Proangiogenic Myeloid Cells

Roberta Mazzieri,[1,2,6] Ferdinando Pucci,[1,2,3,6] Davide Moi,[1,2] Erika Zonari,[1,2] Anna Ranghetti,[1,2] Alvise Berti,[3] Letterio S. Politi,[4] Bernhard Gentner,[2,3] Jeffrey L. Brown,[5] Luigi Naldini,[1,2,3,7,*] and Michele De Palma[1,2,7,*]
[1]Angiogenesis and Tumor Targeting Research Unit
[2]San Raffaele-Telethon Institute for Gene Therapy (HSR-TIGET), Division of Regenerative Medicine, Stem Cells and Gene Therapy San Raffaele Scientific Institute, 20132 Milan, Italy
[3]Vita-Salute San Raffaele University Medical School, 20132 Milan, Italy
[4]Neuroradiology Department, San Raffaele Hospital, 20132 Milan, Italy
[5]AstraZeneca Pharmaceuticals, Waltham, MA 02451, USA
[6]These authors contributed equally to this work
[7]These authors share senior authorship
*Correspondence: depalma.michele@hsr.it (M.D.P.), naldini.luigi@hsr.it (L.N.)
DOI 10.1016/j.ccr.2011.02.005

SUMMARY

Tumor-infiltrating myeloid cells convey proangiogenic programs that counteract the efficacy of antiangiogenic therapy. Here, we show that blocking angiopoietin-2 (ANG2), a TIE2 ligand and angiogenic factor expressed by activated endothelial cells (ECs), regresses the tumor vasculature and inhibits progression of late-stage, metastatic MMTV-PyMT mammary carcinomas and RIP1-Tag2 pancreatic insulinomas. ANG2 blockade did not inhibit recruitment of MRC1$^+$ TIE2-expressing macrophages (TEMs) but impeded their upregulation of *Tie2*, association with blood vessels, and ability to restore angiogenesis in tumors. Conditional *Tie2* gene knockdown in TEMs was sufficient to decrease tumor angiogenesis. Our findings support a model wherein the ANG2-TIE2 axis mediates cell-to-cell interactions between TEMs and ECs that are important for tumor angiogenesis and can be targeted to induce effective antitumor responses.

INTRODUCTION

Among the signaling molecules that regulate the tumor vasculature are members of the vascular-endothelial growth factor (VEGF) pathway, some of which represent validated targets of antiangiogenic therapies (Chung et al., 2010; Kerbel, 2008). However, antiangiogenic treatments targeting the VEGF pathway rarely induce durable tumor responses, both in mice and patients with cancer (Bergers and Hanahan, 2008), and may also favor metastasis in selected tumor models (Ebos et al., 2009; Paez-Ribes et al., 2009). Recently, tumor resistance or recurrence after antiangiogenic therapy has been causally linked to the recruitment of bone marrow (BM)-derived myeloid cells (Shojaei et al., 2007). Damaging the tumor vasculature indeed enhances tumor hypoxia, which in turn upregulates the expression of several myeloid cell chemoattractants (e.g., stromal cell-derived factor-1, SDF1) that rouse the influx of myeloid cells to treated tumors (Bergers and Hanahan, 2008; Chan et al., 2009; Du et al., 2008). Once recruited to the tumors, myeloid cells promote angiogenesis by releasing angiogenic and tissue-remodeling factors (Coffelt et al., 2010a; De Palma et al., 2005), and also stimulate tumor cell intravasation, dissemination, and metastasis (DeNardo et al., 2009; Qian and Pollard, 2010).

Significance

Recent studies showed that antiangiogenic, cytotoxic, and radiation treatments enhance tumor infiltration by bone marrow-derived, proangiogenic cells. The recruited bone marrow-derived cells were shown to promote tumor revascularization and relapse in certain mouse tumor models. Here, we show that targeting the ANG2/TIE2 pathway by a fully humanized anti-ANG2 monoclonal antibody inhibits tumor angiogenesis, growth, and metastasis, and disables the proangiogenic activity of tumor-infiltrating TEMs, thus impeding the emergence of evasive resistance to antiangiogenic therapy. Blocking ANG2 inhibits tumor angiogenesis and growth also in mouse tumor models that were reported to develop resistance to anti-VEGF/VEGFR therapy. Thus, specifically targeting ANG2 may provide an effective antiangiogenic therapy that targets tumor blood vessels while concomitantly disabling rebounds of proangiogenic myeloid cells.

Angiopoietins (ANGs) constitute another important class of angiogenic molecules (Augustin et al., 2009; Huang et al., 2010; Saharinen et al., 2010). ANG2 is upregulated by hypoxia and may trigger angiogenesis via an autocrine loop in endothelial cells (ECs), which express the ANG2 receptor, TIE2. Experimental evidence supports the notion that the ANG2-TIE2 axis promotes angiogenesis in tumors by destabilizing the blood vessels (e.g., by decreasing pericyte coverage) and sensitizing ECs to proliferation signals mediated by other proangiogenic factors, namely VEGF (Augustin et al., 2009; Saharinen et al., 2010). However, in the absence of VEGF, ANG2 promotes EC apoptosis and consequent blood vessel regression (Augustin et al., 2009; Chae et al., 2010; Holash et al., 1999; Saharinen et al., 2010). ANG1, another TIE2 ligand, is known to promote vascular maturation by increasing EC-pericyte interactions (Augustin et al., 2009; Saharinen et al., 2010; Suri et al., 1996). Because the phenotypes of *Angpt1*-deficient and *Angpt2*-overexpressing mice are similar, ANG2 has long been regarded as an antagonist for ANG1, although more recent studies have indicated that ANG2 may function as a context-dependent TIE2 agonist (Augustin et al., 2009; Saharinen et al., 2010). Genetic or pharmacological targeting of ANG2 reduced tumor angiogenesis and delayed the growth of subcutaneous tumors to variable extent in different studies (Brown et al., 2010; Hashizume et al., 2010; Nasarre et al., 2009; Oliner et al., 2004); the role of ANG2 in tumor angiogenesis and growth—and its therapeutic significance as a molecular target—remains controversial and poorly defined (Augustin et al., 2009; Saharinen et al., 2010). Furthermore, the benefits of targeting ANG2 need to be assessed in clinically relevant tumor models, such as spontaneous and metastatic tumors.

Expression of the ANG receptor, TIE2, is not restricted to ECs. TIE2 is weakly expressed by some circulating monocytes and is significantly upregulated upon their homing to tumors and differentiation into a subset of perivascular macrophages (De Palma et al., 2003, 2005, 2008). These TIE2-expressing macrophages (TEMs) have features of M2-polarized tumor-associated macrophages (TAMs) (Mantovani and Sica, 2010), promote both developmental and tumor angiogenesis (Fantin et al., 2010; Pucci et al., 2009), and are required for the formation of tumor blood vessels (De Palma et al., 2003, 2005). Because tumor-infiltrating TEMs promote vascular regrowth following therapy-induced vascular damage (Kioi et al., 2010; Kozin et al., 2010), targeting these cells might increase the efficacy of antiangiogenic treatments by counteracting myeloid cell-mediated angiogenesis and resistance to therapy (Bergers and Hanahan, 2008).

TEMs, but not TIE2$^-$ monocytes, respond to ANG2 stimulation in vitro (Coffelt et al., 2010b; Murdoch et al., 2007; Venneri et al., 2007), suggesting that the ANG2-TIE2 axis may also regulate TEM functions in vivo. We then asked whether targeting the ANG/TIE2 signaling pathway would inhibit tumor angiogenesis and growth also by interfering with TEM's proangiogenic activity.

RESULTS

ANG2 Blockade Inhibits Tumor Growth in Mammary Tumor Models

To specifically neutralize ANG2, we used a fully humanized monoclonal antibody (clone 3.19.3) that efficiently blocks ANG2, but not ANG1, binding to TIE2 (Brown et al., 2010). Biweekly injections of 3.19.3, but not control immunoglobulins (IgGs) or saline (vehicle) alone, inhibited tumor growth by ~50% in MMTV-PyMT transgenic mice, which spontaneously develop aggressive and metastatic mammary carcinomas (Figure 1A; see Figure S1A available online). We observed tumor inhibition after both early (starting at 7 weeks of age) and late (starting at 12 weeks of age) treatment schedules, indicating that ANG2 has a functional role also during late-stage tumorigenesis. Of note the 8-week-long early treatment schedule did not select for resistance to therapy.

In order to obtain synchronized, late-stage tumors, we injected tumor cells derived from 16-week-old MMTV-PyMT mice orthotopically in the third mammary fat pad of syngenic mice. We then treated established tumors (15 days post-tumor cell injection) by either short (2 weeks) or extended (9 weeks) treatment schedules. Both treatment schedules inhibited tumor growth (Figure 1B). Following a short treatment schedule, the tumors remained inhibited for another 2 weeks but then resumed their growth without showing accelerated growth kinetics. Upon an extended treatment schedule, the tumors remained unceasingly inhibited and appeared largely necrotic and fibrotic at the end of the experiments (Figure 1C). Overall, ANG2 blockade inhibited the growth of orthotopic MMTV-PyMT tumors by 70%–80% and extended mouse survival significantly in several independent experiments.

We observed antitumor activity of 3.19.3 also in subcutaneous A431 human carcinomas grown in immunodeficient, CD1 athymic mice (Figure S1B). Taken together, these results indicate that ANG2 blockade inhibits primary tumor growth without eliciting detectable resistance to the treatment, even in late-stage tumors or upon prolonged treatment schedules.

ANG2 Blockade Regresses the Vasculature and Inhibits Angiogenesis in Mammary Tumor Models

We then analyzed angiogenesis in spontaneous and orthotopic MMTV-PyMT carcinomas (Figures 2A and 2B), as well as subcutaneously growing A431 human carcinomas (Figure S2A). We measured vascular parameters by immunofluorescence staining (IFS) and confocal microscopy of tumor sections (orthotopic MMTV-PyMT model) and flow cytometry of tumor cell suspensions obtained from multiple tumor biopsies (spontaneous MMTV-PyMT model).

In orthotopic MMTV-PyMT (Figure 2A) and subcutaneous A431 (Figure S2A) carcinomas treated according to a short schedule, 3.19.3 greatly reduced the relative tumor vascular area (measured by IFS of CD31$^+$ blood vessels). In spontaneous MMTV-PyMT tumors treated according to a late schedule, 3.19.3 significantly reduced the proportion of viable ECs among tumor-derived cells (measured by flow cytometry) (Figures 2B; Figure S2B). Together, these data indicate profound antiangiogenic activity of 3.19.3 in the tumor models tested.

Although 3.19.3-treated tumors contained vascular-like structures heavily coated by NG2$^+$ pericytes, the inner EC lining was often discontinuous or even absent (Figure 2A; Movies S1 and S2). This feature, together with the lower ratio of CD31$^+$/NG2$^+$ area (Figure 2B), strongly suggested regression of established blood vessels in 3.19.3-treated tumors. Consistent with impaired angiogenesis and vascular regression, 3.19.3 reduced tumor perfusion and dramatically increased tumor hypoxia (Figure 2C) and necrosis (Figures 2A and 2C). Of note, large hypoxic

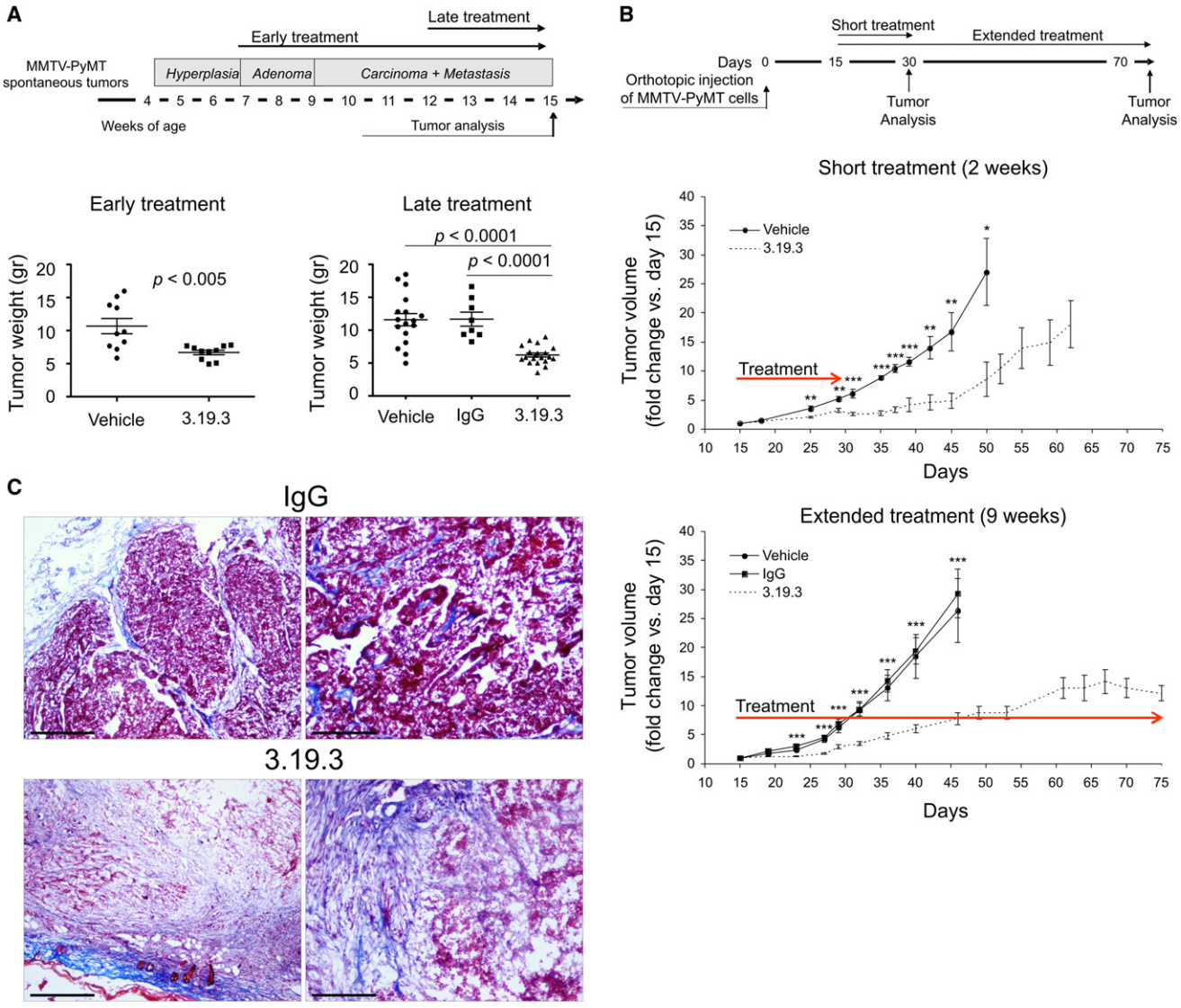

Figure 1. ANG2 Blockade Inhibits Tumor Growth in MMTV-PyMT Mammary Tumor Models

(A) Tumor growth in transgenic MMTV-PyMT mice. Top panel shows schematics of the early and late-treatment trials. Bottom panels illustrate tumor weight (mean tumor weight ± SEM) of 15-week-old mice treated according to early (one experiment; n = 10/group) or late (three experiments combined; n = 8–19/group) schedules. Each dot in the plots corresponds to one mouse bearing multiple mammary tumors. Statistical analyses by unpaired Student's t test.

(B) Tumor growth in mice carrying orthotopic, late-stage MMTV-PyMT mammary tumors. Top panel shows schematics of the experimental design. Middle and bottom panels illustrate tumor growth (mean tumor volume ± SEM, shown as fold-change versus first day [day 15] of treatment) in short (middle; n = 8 mice/group) and extended (bottom; n = 10–12 mice/group) treatment trials. Statistical analyses were performed on actual tumor volume data by unpaired Student's t test. *, $p < 0.01$; **, $p < 0.005$; ***, $p < 0.001$.

(C) Masson's trichrome staining of orthotopic, late-stage MMTV-PyMT mammary tumors treated according to an extended (9 weeks) treatment schedule. Collagen's blue staining demonstrates abundant fibrotic tissue and scant tumor cells in 3.19.3-treated tumors (day 78). Left panels show tumor periphery. Scale bars, 600 μm (left panels) and 300 μm (right panels). Images are representative of five 3.19.3-treated (day 78) and three control IgG-treated (day 48) tumors.

or necrotic tumor areas were frequently observed in proximity to $CD31^+$ blood vessels (Figure 2C) or $NG2^+$ sheaths lacking EC lining (Figure 2A) in the tumors of 3.19.3-treated but not untreated mice.

ANG2 Blockade Inhibits Progression and Angiogenesis of Late-Stage Pancreatic Islet Tumors

It has been reported that late-stage RIP1-Tag2 pancreatic islet tumors are insensitive to VEGF/VEGFR2 blockade (Casanovas et al., 2005; Shojaei et al., 2008). We then investigated whether late-stage islet tumors are sensitive to ANG2 blockade following a treatment schedule similar to that used by Hanahan and coworkers (Casanovas et al., 2005). To this aim we treated 12-week-old, RIP1-Tag2 mice with biweekly injections of either vehicle or 3.19.3 for 3.5 weeks (Figure 3A). The mice were euthanized at 15.5 weeks of age, when most of the vehicle but not 3.19.3-treated mice showed signs of distress (data not shown). We also euthanized a group of untreated mice at 12 weeks of

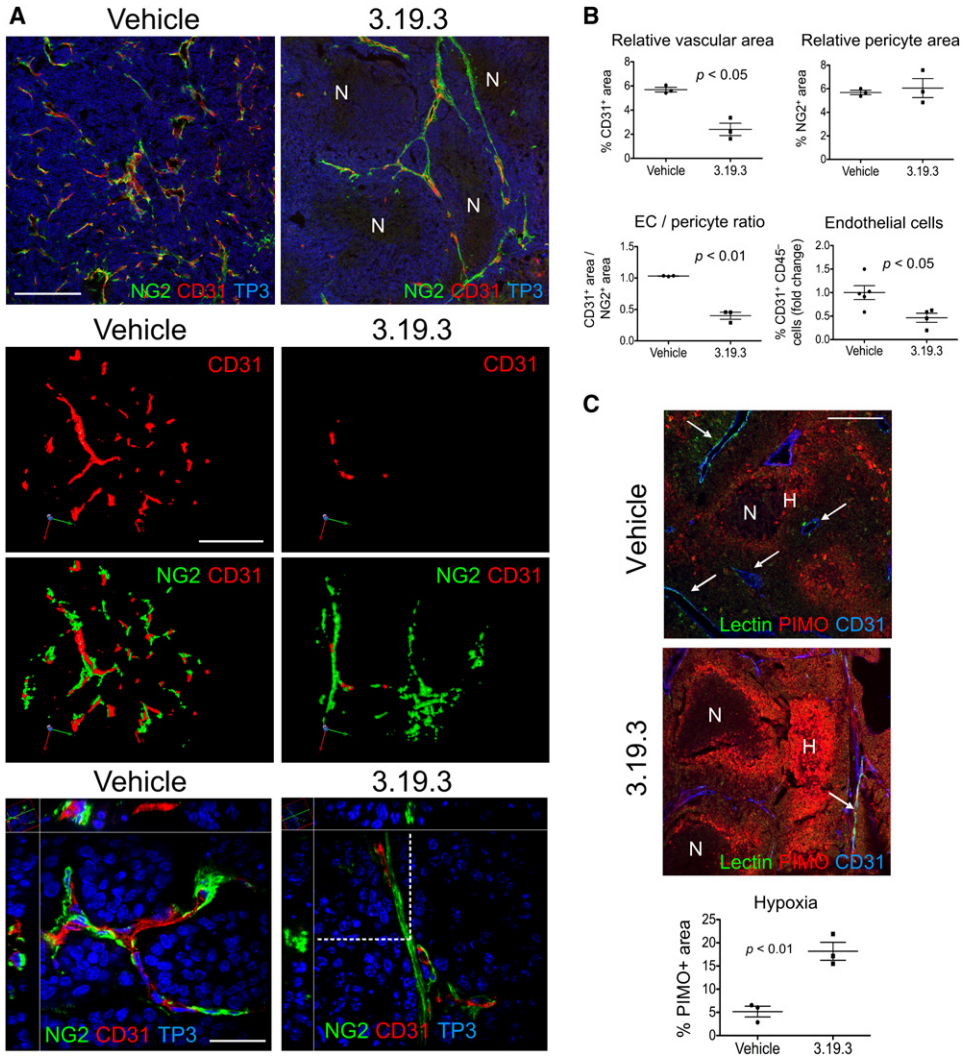

Figure 2. ANG2 Blockade Regresses the Vasculature and Inhibits Angiogenesis in MMTV-PyMT Mammary Tumor Models

(A) NG2 (green) and CD31 (red) immunostaining, and TO-PRO-3 (TP3) nuclear staining (blue) of orthotopic, late-stage MMTV-PyMT mammary tumors treated according to a short (2 weeks) schedule and analyzed immediately after discontinuation of therapy. Top panels show confocal images of representative tumor sections. N, necrotic tumor areas. Scale bar, 300 μm. Middle panels show images of three-dimensional models obtained by surface rendering of the confocal Z stacks, after superimposition of multiple confocal planes (section thickness, 16 μm). Scale bar, 150 μm. Bottom panels show superimposition of multiple confocal Z stacks imaging individual blood vessels. Scale bar, 50 μm. Results are representative of two independent experiments and ten tumors per group analyzed.

(B) Morphometric (Relative vascular area; Relative pericyte area; EC/pericyte ratio) and flow cytometry (Endothelial cells) analyses of angiogenesis in orthotopic (morphometric analyses) and spontaneous (flow cytometry) MMTV-PyMT mammary tumors. Each dot in the plots corresponds to one tumor; scatter plots show mean values ± SEM. Statistical analyses by unpaired Student's t test.

(C) Top panels illustrate lectin (green), hypoxia (PIMO; red), and CD31 (blue) immunostaining of orthotopic, late-stage MMTV-PyMT mammary tumors treated according to a short (2 weeks) schedule. N, necrotic tumor areas; H, hypoxic areas; arrows indicate lectin$^+$/CD31$^+$ perfused blood vessels. Scale bar, 150 μm. Results are representative of two independent experiments and eight tumors per group analyzed. Bottom panel shows quantification of hypoxia in three representative tumors (mean percentage [%] of PIMO$^+$ area ± SEM). Statistical analyses by unpaired Student's t test.

age (t0) in order to obtain pancreatic tissue at a time point coinciding with the initiation of therapy (Figure 3A).

Clone 3.19.3 significantly reduced the mean tumor area (versus vehicle; Figure 3A) calculated by measuring each of the islet tumors scored in the largest pancreatic section (28–72 tumors per section; Figure S3). Of note, large tumors exceeding 0.5 mm^2 of area were significantly fewer in 3.19.3-treated than control mice (Figure 3A; Figure S3), indicating that ANG2 blockade effectively inhibited the progression of advanced tumors in RIP1-Tag2 mice. Furthermore, 3.19.3 did not increase local invasion by islet tumors, as shown by the similar proportions of noninvasive, partially invasive (IC1), or entirely invasive (IC2) tumors (Ebos et al., 2009; Paez-Ribes et al., 2009) in 3.19.3-treated and control mice (Figure 3B).

We then studied tumor angiogenesis. Clone 3.19.3 greatly reduced the relative tumor vascular area, measured by IFS of

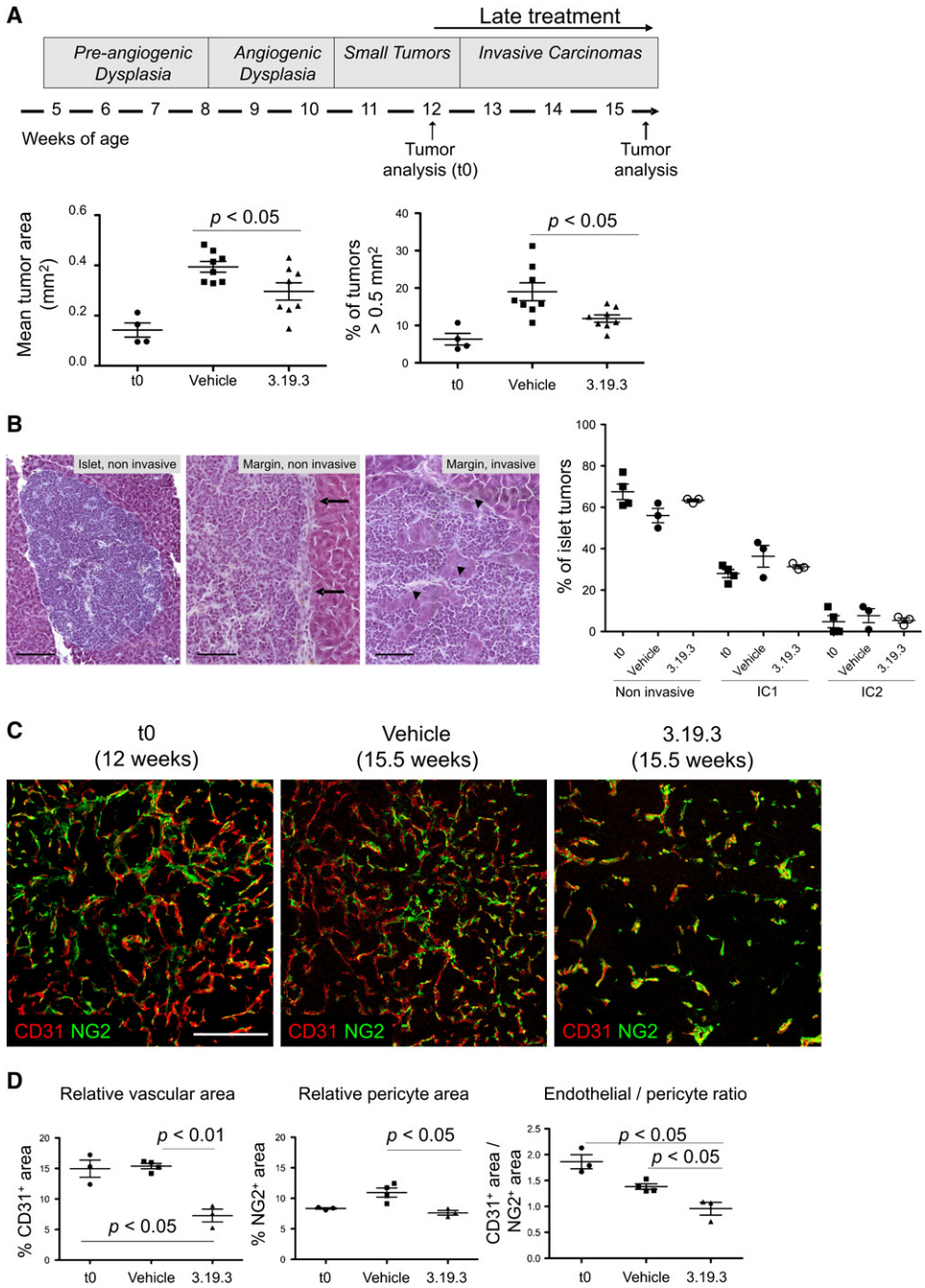

Figure 3. ANG2 Blockade Inhibits Progression and Angiogenesis of Late-Stage, RIP1-Tag2 Pancreatic Islet Tumors

(A) Top panel shows schematics of the late treatment trial. Bottom-left panel illustrates mean tumor area (±SEM; two independent experiments combined; n = 4–8/group). Bottom-right panel shows proportion (%) of tumors exceeding 0.5 mm^2 of area (mean value ± SEM; two independent experiments combined; n = 4–8/group). Each dot in the plots corresponds to one mouse, of which multiple islet tumors contained in the largest pancreatic section were analyzed. Statistical analyses by unpaired Student's t test.

(B) Left panels illustrate hematoxylin and eosin staining (H&E) of pancreatic sections showing examples of noninvasive (left and middle panels) and invasive (right panel) islet tumors. Scale bars, 300 μm (left panel) and 150 μm (middle and right panels). Right panel illustrates proportion (%; mean value ± SEM) of tumors with noninvasive, partially invasive (IC1) or entirely invasive (IC2) margins. Each dot in the plots corresponds to one mouse, of which multiple islet tumors contained in the largest pancreatic section were analyzed.

(C) NG2 (green) and CD31 (red) immunostaining of islet tumors. Scale bar, 150 μm. Results are representative of two independent experiments and three to four mice per group analyzed.

(D) Morphometric analyses of angiogenesis (Relative vascular area; Relative pericyte area; Endothelial / pericyte ratio; mean values ± SEM) in islet tumors analyzed at the indicated time points. Each dot in the plots corresponds to one mouse, of which multiple tumors were analyzed. Statistical analyses by unpaired Student's t test.

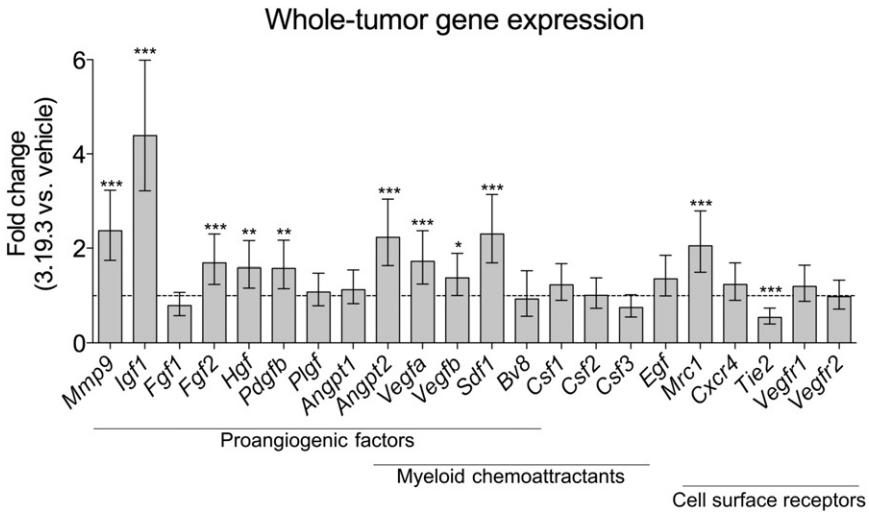

Figure 4. ANG2 Blockade Upregulates the Expression of Proangiogenic Genes in Mammary Tumors

Gene expression by qPCR in whole-tumor lysates obtained from spontaneous MMTV-PyMT tumors treated with 3.19.3 (mean fold change over reference value [vehicle]). For each mouse (n = 3–4 mice/group), two to three small tumor biopsies were obtained and pooled together. Error bars represent 95% confidence interval (1.96 × SEM). *Gapdh* and *Hprt* were used as reference genes. Genes differentially expressed between 3.19.3- and vehicle-treated tumors are indicated by the asterisks (*, $p < 0.05$; **, $p < 0.01$; ***, $p < 0.001$).

CD31$^+$ blood vessels (Figures 3C and 3D). Of note, the relative tumor vascular area was similar in t0 (12 weeks of age) and vehicle-treated (15.5 weeks of age) mice but was reduced by more than 50% in 3.19.3-treated mice (15.5 weeks of age). As seen in MMTV-PyMT carcinomas, 3.19.3 enhanced pericyte coverage of tumor blood vessels (Figures 3C and 3D). These data indicate profound antiangiogenic activity of ANG2 blockade in late-stage, pancreatic islet tumors.

ANG2 Blockade Upregulates the Expression of Proangiogenic Genes in Mammary Tumors

We then analyzed the expression of a panel of angiogenesis-associated and myeloid cell-growth factor/chemoattractant genes by qPCR (Figure S4) in tumor lysates obtained from spontaneous MMTV-PyMT carcinomas treated according to a late schedule (Figure 1A). Although none of the investigated genes showed major changes, the proangiogenic genes *Angpt2*, *Fgf2*, *Hgf*, *Pdgfb*, *Vegfa*, *Vegfb*, *Mmp9*, and *Sdf1* were all upregulated in 3.19.3-treated versus untreated tumors (Figure 4). Of note, enhanced expression of *Fgf2*, *Sdf1*, and *Hgf* has been previously associated with tumor resistance to various antiangiogenic or radiation treatments (Casanovas et al., 2005; Kozin et al., 2010; Shojaei et al., 2010).

Whereas *Sdf1*, *Vegfa*, and *Angpt2* were slightly upregulated, other myeloid cell-growth factor/chemoattractant genes (e.g., *Bv8*/prokinecitin-1, *Csf1*/M-CSF, *Csf2*/GM-CSF, and *Csf3*/G-CSF) did not show significant changes in 3.19.3-treated versus untreated tumors (Figure 4). Interestingly, *Tie2* was significantly downregulated, whereas the expression of other EC receptors (e.g., *Vegfr1*, *Vegfr2*, and *Cxcr4*) was similar in 3.19.3-treated versus untreated tumors (Figure 4). *Igf1*, which is an EC antiapoptotic/survival factor highly expressed by TEMs (Pucci et al., 2009), was strongly upregulated in 3.19.3-treated versus untreated tumors. In summary these data suggest that mammary tumors upregulate, albeit marginally, the expression of several proangiogenic genes following ANG2 blockade; nevertheless, the treated tumors did not show evidence for rebound angiogenesis (Figures 2A–2C) or growth resistance (Figures 1A–1C).

ANG2 Blockade Does Not Inhibit Tumor Infiltration by TEMs but Impedes Their Association with Blood Vessels

We previously showed that TEMs can be distinguished from TIE2$^-$ TAMs by their cell surface marker profile (TEMs: CD11b$^+$/F4/80$^+$/MRC1^{high}/CD11c$^-$; TIE2$^-$ TAMs: CD11b$^+$/F4/80$^+$/MRC1$^{low/-}$/CD11c$^+$) (Pucci et al., 2009) and perivascular location (De Palma et al., 2005). Because TIE2$^-$ TAMs express higher amounts of classic proinflammatory genes than TEMs (Pucci et al., 2009), here we refer to the former as "inflammatory TAMs."

ANG2 was previously shown to be a TEM chemoattractant (Coffelt et al., 2010b; Murdoch et al., 2007; Venneri et al., 2007). We then asked whether ANG2 blockade inhibited TEM recruitment to the tumors. We found that MMTV-PyMT carcinomas contained substantial numbers of MRC1$^+$ TEMs (Figures 5A and 5B). Unexpectedly, ANG2 blockade enhanced tumor infiltration by MRC1$^+$ TEMs, but not inflammatory TAMs or total CD11b$^+$ myeloid cells, both in spontaneous (Figure 5A; Figure S5A) and orthotopic (Figure 5B) MMTV-PyMT tumors. The enhanced recruitment of MRC1$^+$ TEMs in 3.19.3-treated tumors may be fostered by increased tumor hypoxia and/or expression of SDF1 (Figures 2C and 4), which are known TEM-recruiting signals (Kioi et al., 2010; Kozin et al., 2010). Interestingly, whereas in control tumors the MRC1$^+$ cells were mostly associated with CD31$^+$ blood vessels (a typical TEM feature), in 3.19.3-treated tumors these cells were more homogeneously spread in the tumor mass and frequently disengaged from the blood vessels (Figures 5A and 5B).

ANG2 blockade did not increase MRC1$^+$ TEM infiltration in RIP1-Tag2 islet tumors but, similar to findings in MMTV-PyMT carcinomas, displaced them from the blood vessels (Figure 5C). This was true also in the scant tumor regions characterized by a relatively high vascular area (Figure S5B). Together, these data suggest that ANG2 is not required for TEM recruitment to the tumors but regulates their interaction with angiogenic blood vessels.

ANG2 Blockade Impedes Tumor TEM Upregulation of *Tie2*

Because 3.19.3 strongly inhibited tumor angiogenesis, the finding of increased numbers of MRC1$^+$ TEMs in 3.19.3-treated

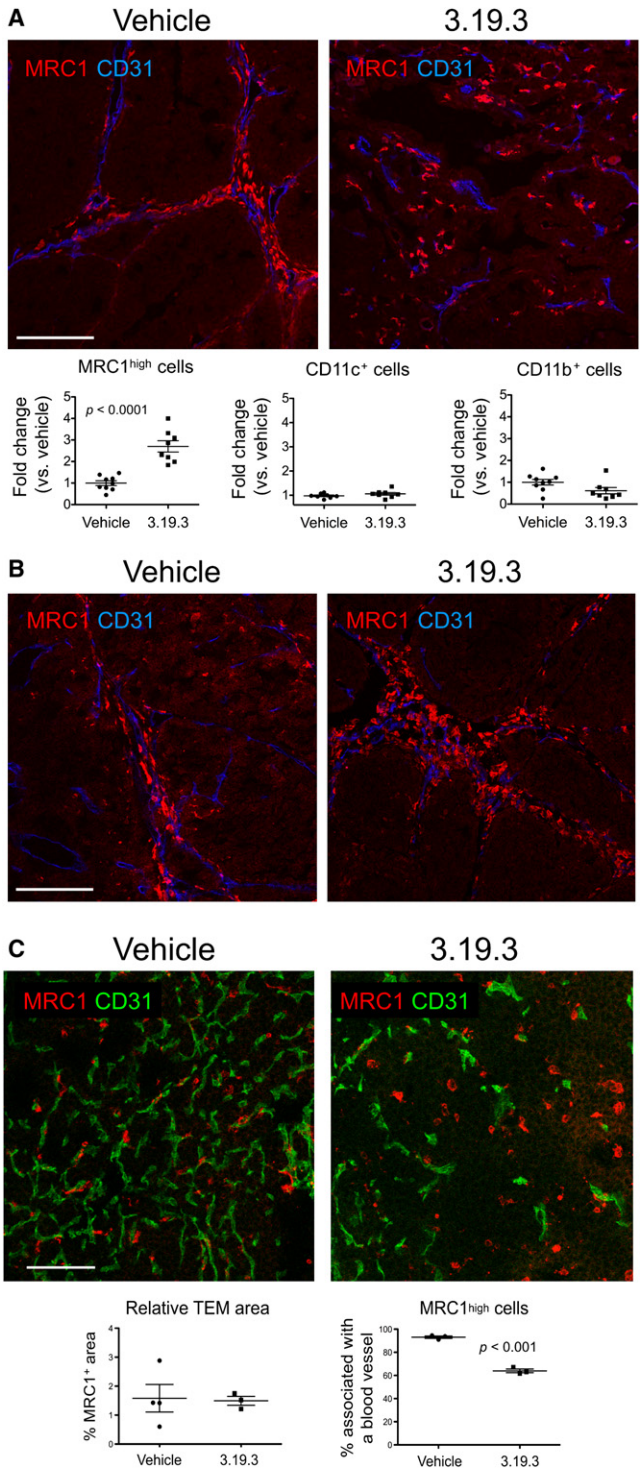

Figure 5. ANG2 Blockade Does Not Inhibit Tumor Infiltration by TEMs but Impedes Their Association with Blood Vessels

(A) Top panels show MRC1 (red) and CD31 (blue) immunostaining of spontaneous, late-stage MMTV-PyMT mammary tumors treated according to a late schedule and analyzed at 15 weeks of age (see Figure 1A). Scale bar, 150 μm. Results are representative of three independent experiments and three to five tumors per group analyzed. Bottom panels illustrate flow cytometry analyses of myeloid cell infiltrates in tumors treated as above (mean frequency of tumor-derived cells ± SEM, shown as fold change versus reference [vehicle]). Each dot in the plots corresponds to one mouse; tumor samples were obtained from three independent experiments. Statistical analyses by unpaired Student's t test.

(B) MRC1 (red) and CD31 (blue) immunostaining of orthotopic, late-stage MMTV-PyMT mammary tumors treated according to a short schedule (see Figure 1B) and analyzed 2 weeks after the first treatment. Scale bar, 150 μm. Results are representative of two independent experiments and ten tumors per group analyzed.

(C) Top panels show MRC1 (red) and CD31 (green) immunostaining of late-stage RIP1-Tag2 islet tumors treated according to a late schedule and analyzed at 15.5 weeks of age (see Figure 3A). Scale bar, 100 μm. Results are representative of two independent experiments, three to four mice per group and several tumors analyzed. Bottom panels show morphometric analyses (mean values ± SEM) of MRC1$^+$ cell infiltration (left) and association with blood vessels (right) in islet tumors treated as above. Each dot in the plots corresponds to one mouse, of which multiple tumors were analyzed. Statistical analyses by unpaired Student's t test.

MMTV-PyMT carcinomas appeared paradoxical in view of the proangiogenic activity of these cells. In order to investigate whether ANG2 blockade altered gene expression in TEMs, we isolated TEMs (7AAD$^-$/CD11b$^+$/CD31^{low}/MRC1^{high}/CD11c$^-$), inflammatory TAMs (7AAD$^-$/CD11b$^+$/CD31^{low}/MRC1$^{low/-}$/CD11c$^+$), and ECs (7AAD$^-$/CD31^{high}/CD11b$^-$) from both 3.19.3-treated and untreated, orthotopic MMTV-PyMT carcinomas, and analyzed the expression of a panel of genes of interest (Figure S4) in the sorted cells. In agreement with our previous gene expression studies performed in the N202 mammary tumor model (Pucci et al., 2009), *Tie2*, *Igf1*, *Sdf1*, and *Mrc1* were all highly upregulated in TEMs versus inflammatory TAMs isolated from untreated MMTV-PyMT tumors (Figure 6A; Figure S4). Therefore, the higher expression level of *Igf1*, *Mrc1*, and *Sdf1* in whole mammary tumor lysates of 3.19.3-treated (versus untreated) mice (Figure 4) is consistent with their enhanced infiltration by TEMs (Figures 5A and 5B; Figure S5A).

Interestingly, the expression level of *Tie2*—but not other TEM-distinguishing genes—was significantly lower (8- to 10-fold in four independent experiments) in TEMs isolated from 3.19.3-treated than control tumors (Figure 6B; Figure S4; data not shown). Because *Tie2* is strongly upregulated in TEMs locally in the tumor microenvironment (De Palma et al., 2008), these data strongly suggested that neutralization of ANG2 had impeded the upregulation of TIE2 in tumor-infiltrating TEMs. On the other hand, ANG2 blockade did not change the expression level of any of the investigated genes in inflammatory TAMs (Figures 6C; Figure S4). Except for *Sdf1*, which was upregulated, none of the genes analyzed in ECs (including *Tie2*) displayed significant changes following ANG2 blockade (Figures 6D; Figure S4).

To verify that, regardless of their differential expression level of *Tie2*, the MRC1$^+$ cells represented bona fide TEMs in both 3.19.3-treated and untreated tumors, we transplanted lethally irradiated, 6-week-old MMTV-PyMT mice with *Tie2*-GFP BM cells (De Palma et al., 2005) and analyzed the tumors at 15 weeks of age after a late treatment schedule (Figure S6). Anti-GFP IFS of tumor sections specifically marked the MRC1$^+$ cells and labeled similar proportions of these cells in 3.19.3- and vehicle-treated mice (Figure S6). Together with the gene expression data in Figure 6B, these results indicate that the MRC1$^+$

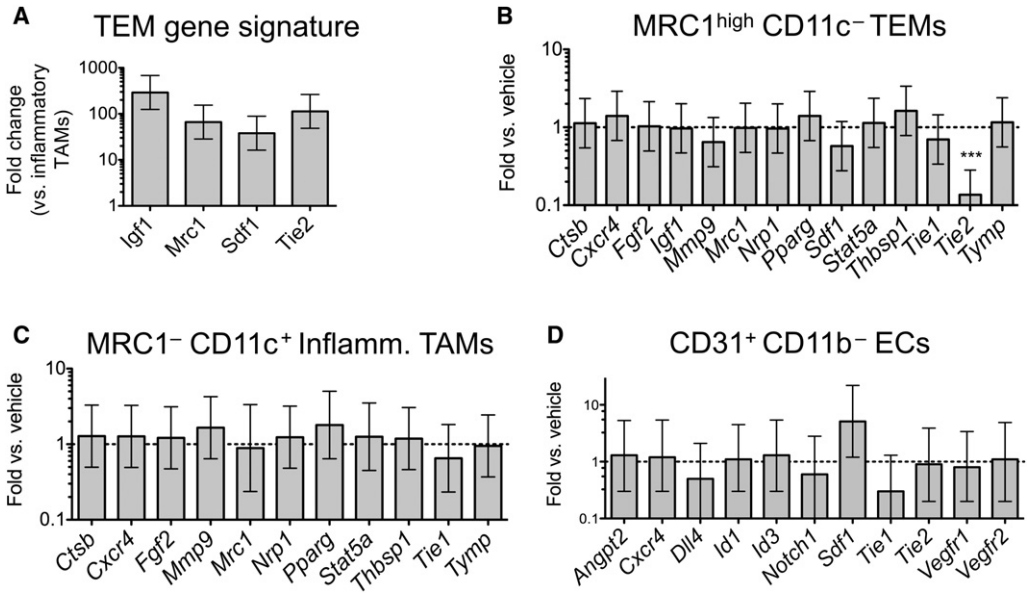

Figure 6. ANG2 Blockade Impedes Tumor TEM Upregulation of *Tie2*

(A) Gene expression by qPCR in TEMs and inflammatory TAMs isolated from untreated, orthotopic MMTV-PyMT tumors (mean fold change over reference value [inflammatory TAMs]; n = 2) analyzed 4 weeks post-tumor injection. Error bars represent 95% confidence interval (1.96 × SEM); *β2 m* was used as reference gene. (B–D) Gene expression by qPCR in TEMs (B; n = 2), inflammatory TAMs (C; n = 2), and ECs (D; n = 3) isolated from orthotopic, late-stage MMTV-PyMT tumors treated with 3.19.3 according to a short schedule (mean fold change over reference value [vehicle]). Error bars represent 95% confidence interval (1.96 × SEM); *β2 m* was used as reference gene. ***, $p < 0.001$. The expression of *Tie2* in TEMs was further analyzed in two additional experiments and confirmed to be significantly lower ($p < 0.001$) in 3.19.3-treated versus vehicle-treated tumors.

cells of 3.19.3-treated tumors maintain a distinguishing TEM phenotype but fail to upregulate *Tie2*, a molecular switch that could be required to promote TEM association with angiogenic blood vessels and execution of their proangiogenic activity.

Conditional *Tie2* Gene Knockdown in TEMs Reduces Tumor Angiogenesis and Perfusion in Mammary Tumors

We then asked whether the impeded upregulation of *Tie2* in TEMs contributed to the antiangiogenic activity of ANG2 blockade in MMTV-PyMT carcinomas. To address this question we silenced TIE2 specifically in the mature hematopoietic cells of tumor-bearing mice. We previously described the delivery of small interfering RNA (siRNA) using microRNA (miRNA)-based lentiviral vectors (LVs) (Amendola et al., 2009). To silence TIE2, we replaced the stem sequence of miR-223 with validated siRNA sequences targeting *Tie2* and obtained the artificial miRNA, amiR(*Tie2*); we also generated a control amiR targeting *Luciferase*, amiR(*Luc*) (Amendola et al., 2009). To enable inducible gene silencing, we here combined two separate LVs (Figure 7A). In the first vector (LV1), the amiR is placed downstream to a tetracycline-responsive element (TRE)-containing promoter, which also controls the expression of a marker gene (orange fluorescent protein, OFP). In the second vector (LV2), a reverse tetracycline transactivator (rtTA-m2) is placed under the control of the ubiquitously active phosphoglycerate kinase (*PGK*) promoter (*PGK*-rtTA). In order to suppress rtTA expression and, consequently, *Tie2* gene knockdown in hematopoietic stem cells (HSCs), which require TIE2 for their maintenance in the stem cell niche (Arai et al., 2004), we modified the rtTA expression cassette by incorporating target sequences for miR-126 (miR-126T) in the UTR. By this strategy, rtTA expression is suppressed specifically in HSCs via endogenous miRNA-mediated mRNA degradation because only HSCs express high-level miR-126 among hematopoietic-lineage cells (Gentner et al., 2010). We then generated FVB/*PGK*-rtTA-miR-126T (LV2) transgenic mice by LV-mediated transgenesis, as previously described (De Palma et al., 2005), and used them as hematopoietic stem/progenitor cell (HS/PC) donors for ex vivo LV1 transduction and transplantation. We validated the inducible gene knockdown platform both in vitro and in vivo, showing: (i) absence of amiR-induced cell toxicity and counterselection (Figures S7A and S7B) and lack of saturation of the endogenous miRNA pathway (Figure S7C) in vitro; (ii) efficient and doxycycline-dependent amiR expression in HS/PCs ex vivo (Figures S7D and S7E), circulating monocytes (Figure S7F), and tumor-infiltrating TEMs (Figure S7G) in vivo; and (iii) virtually complete detargeting of amiR expression from primitive HSCs in vivo (Figures S7H and S7I). Furthermore, expression of the amiR (*Tie2*) did not perturb whole blood cell counts (Figure S7J), leukocyte (Figure S7K) and monocyte (Figure S7L) subsets, nor did it induce counterselection of LV1-transduced cells (Figure S7M) in the transplanted mice (compared with amiR(*Luc*) mice).

To study the effects of *Tie2* gene knockdown in a model of spontaneous tumorigenesis, we generated MMTV-PyMT/amiR (*Tie2*) and MMTV-PyMT/amiR(*Luc*) mice (two independent experiments; n = 12–14 mice/group) by HS/PC transduction and transplantation, as described above. We treated the mice with doxycycline starting at 4 weeks post-transplant (9.5 weeks of age), when the angiogenic switch and malignant conversion occur in this tumor model (De Palma et al., 2008; Lin et al.,

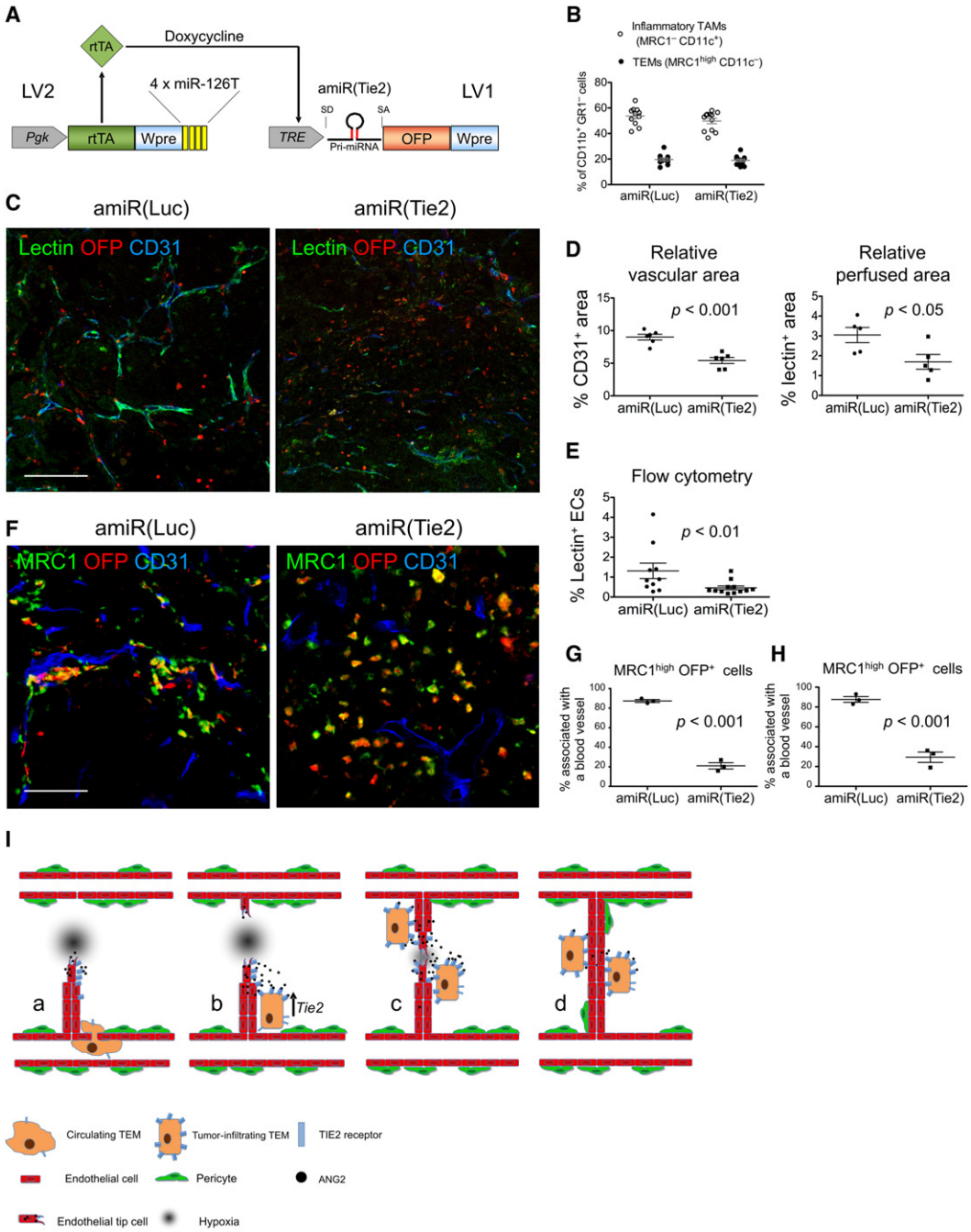

Figure 7. Conditional *Tie2* Gene Knockdown in TEMs Reduces Tumor Angiogenesis and Impedes TEM Association with Blood Vessels

(A) Schematics of the LV constructs used for *Tie2* gene knockdown in BM-derived cells.

(B) Flow cytometry analyses of mononuclear phagocyte infiltrates (MRC1^{high}/CD11c^{-} TEMs and MRC1^{low}/CD11c^{+} inflammatory TAMs) in tumors of MMTV-PyMT/amiR(*Tie2*) and MMTV-PyMT/amiR(*Luc*) mice. Each dot in the plot corresponds to one mouse (n = 11–12 mice/group); results are shown as mean values ± SEM. Two independent experiments are shown after combining the data.

(C) Lectin (green), OFP (red), and CD31 (blue) immunostaining of tumor sections of MMTV-PyMT/amiR(*Tie2*) and MMTV-PyMT/amiR(*Luc*) mice. Scale bar, 150 μm. Results are representative of two independent experiments and 11–12 tumors/group analyzed. For each tumor, three to five sections were analyzed.

(D) The plots show mean values ± SEM of morphometric analyses of angiogenesis in tumors of MMTV-PyMT/amiR(*Tie2*) and MMTV-PyMT/amiR(*Luc*) mice. Each dot indicates one individual tumor; for each tumor, three to five sections were analyzed. Statistical analyses by unpaired Student's t test.

(E) The plot shows mean values ± SEM of lectin^{+}CD31^{+}CD45^{-} ECs in tumors of MMTV-PyMT/amiR(*Tie2*) and MMTV-PyMT/amiR(*Luc*) mice. Each dot indicates one individual mouse; for each mouse, two to three tumor biopsies were obtained and pooled together before analysis. Statistical analyses by unpaired Student's t test.

(F) MRC1 (green), OFP (red), and CD31 (blue) immunostaining of tumor sections of MMTV-PyMT/amiR(*Tie2*) and MMTV-PyMT/amiR(*Luc*) mice. Scale bar, 75 μm. Results are representative of two independent experiments and ten tumors per group analyzed. For each tumor, three to five sections were analyzed. OFP^{+}MRC1^{high} TEMs appear yellow, untransduced MRC1^{high} TEMs appear green, and OFP^{+}MRC1^{-} cells represent BM-derived cells distinct from TEMs.

2006). We euthanized the mice at 15 weeks of age and analyzed their tumors by flow cytometry and IFS of frozen sections.

The frequency of TEMs and inflammatory TAMs among the tumor-infiltrating CD11b$^+$/Gr1$^-$ myelomonocytic cells was similar in MMTV-PyMT/amiR(*Tie2*) and MMTV-PyMT/amiR (*Luc*) mice (Figure 7B), indicating that *Tie2* gene knockdown did not detectably affect TEM recruitment to the tumors. However, when we analyzed tumor angiogenesis, we observed significant differences between MMTV-PyMT/amiR(*Tie2*) and MMTV-PyMT/amiR(*Luc*) mice (Figures 7C and 7D). The CD31$^+$ blood vessels of amiR(*Tie2*) tumors appeared smaller, fewer, and less perfused (lectin$^+$) than in the controls (Figure 7C). Both the CD31$^+$ and lectin$^+$ relative vascular area, measured by IFS of tumor sections, were significantly lower in amiR(*Tie2*) than amiR(*Luc*) mice (Figure 7D), indicating decreased angiogenesis and, possibly, increased vessel immaturity or collapse. Flow cytometric analyses of tumor cell suspensions confirmed the lower proportion of lectin$^+$/CD31$^+$/CD45$^-$ ECs in the tumors of amiR(*Tie2*) mice (Figure 7E). We observed decreased angiogenesis/perfusion also in FVB/amiR(*Tie2*) mice either challenged with orthotopic MMTV-PyMT (Figure S7N) or subcutaneous N202 (Figure S7O) mammary carcinomas. These data indicate that *Tie2* knockdown by RNAi and, consequently, its impeded upregulation in tumor-infiltrating TEMs reduces tumor angiogenesis and blood vessel functionality in mammary tumor models.

Conditional *Tie2* Gene Knockdown in TEMs Impedes Their Association with Tumor Blood Vessels

We noted that the distribution of OFP$^+$MRC1$^+$ cells differed in the tumors of amiR(*Tie2*) and amiR(*Luc*) mice, both in spontaneous (Figures 7F and 7G) and orthotopic (Figure 7H) MMTV-PyMT tumor models. Indeed, there were fewer OFP$^+$MRC1$^+$ TEMs associated with CD31$^+$ tumor blood vessels in amiR(*Tie2*) than amiR(*Luc*) mice (Figures 7G and 7H), suggesting that *Tie2* knockdown in TEMs had hampered their ability to associate with angiogenic blood vessels. Together with the ANG2 blockade data shown above, these findings indicate that TIE2 expression by TEMs is required for their association with angiogenic blood vessels, and that disrupting such association (either by interfering with *Tie2* expression in TEMs, or by neutralizing the TIE2 ligand, ANG2) limits the formation of intratumoral vascular networks (Figure 7I).

Whereas *Tie2* knockdown in TEMs was sufficient to significantly decrease angiogenesis in multiple tumor models (Figures 7C–7E; Figures S7N and 7O), it failed to reproducibly inhibit tumor growth (data not shown). However, it should be noted that the frequency of OFP$^+$ TEMs ranged from 50% to 90% (average: 70%) in the tumors of both amiR(*Tie2*) and amiR(*Luc*) mice (Figure S7P), indicating that *Tie2* gene knockdown had occurred in the majority but not all tumor-infiltrating TEMs.

ANG2 Blockade Inhibits Spontaneous and Preestablished Mammary Tumor Metastasis

We then asked whether angiogenesis inhibition following ANG2 blockade affected tumor cell dissemination and outgrowth of pulmonary metastases in MMTV-PyMT transgenic mice. We analyzed the lungs of 3.19.3-treated and control mice from either early (one experiment; 8 weeks of treatment; n = 10 mice/group) or late (two independent experiments; 3 weeks of treatment; n = 10 mice/group) treatment trials. Both in early and late treatment trials, 3.19.3 effectively inhibited spontaneous metastasis in MMTV-PyMT mice (Figures 8A and 8B; Figure S8). In order to discriminate direct versus indirect effects of 3.19.3 on metastasis formation, we used a model in which metastatic growth is independent of the primary tumor. To this aim we intravenously injected tumor cells obtained from late-stage MMTV-PyMT carcinomas into wild-type mice; by this approach, pulmonary metastases form in the absence of a primary tumor. Starting at 1 day after tumor cell inoculation, mice were treated with 3.19.3 for 25 days or left untreated, and the lungs were analyzed thereafter. Whereas 3.19.3 did not significantly decrease the number of metastases in the lung parenchyma, it dramatically inhibited the progression from a micro- to a macrometastatic stage, as shown by volumetric analysis of the pulmonary tumor burden (Figure 8C). These data provide direct evidence that ANG2 blockade not only inhibits primary tumor growth and its metastatic dissemination but also directly suppresses the growth of established metastases.

DISCUSSION

Here, we demonstrate that ANG2 blockade: (i) inhibits angiogenesis and induces vascular regression in multiple tumor models, including tumors that are prone to develop resistance to anti-VEGF/VEGFR therapy; (ii) inhibits tumor growth in multiple tumor models, including late-stage spontaneous tumors; (iii) limits the metastatic dissemination of primary tumors and the outgrowth of established metastasis; and (iv) impedes, in tumor-infiltrating TEMs, the transcriptional upregulation of *Tie2*, which is required for their association with tumor blood vessels and proangiogenic activity.

Sustained Antiangiogenic and Antitumor Activity of ANG2 Blockade

We neutralized ANG2 using an ANG2-specific monoclonal antibody (3.19.3) that potently binds ANG2 with at least 500-fold greater affinity compared with ANG1 (Brown et al., 2010). Clone 3.19.3 markedly reduced the relative tumor vascular area in each tumor model tested, including spontaneous MMTV-PyMT mammary and RIP1-Tag2 pancreatic islet tumors. In these tumor models, ANG2 neutralization increased pericyte coverage of the remnant blood vessels, similar to previous findings in

(G and H) Analysis of OFP$^+$MRC1^{high} TEM/CD31$^+$ blood vessel association in tumors of amiR(*Tie2*) and amiR(*Luc*) mice (G, spontaneous MMTV-PyMT tumors; H, orthotopic MMTV-PyMT tumors grown in FVB mice). Individual OFP$^+$MRC1^{high} TEMs were scored as either associated or not with CD31$^+$ blood vessels. Histograms show mean values (±SEM) of the percentage of OFP$^+$MRC1^{high} TEMs associated with CD31$^+$ blood vessels. In (G), data were obtained from three mice per group and two tumors per mouse; in (H), data were obtained from three tumors per group. Statistical analyses by unpaired Student's t test.

(I) TEM-EC interactions mediated by ANG2-TIE2 promote vascular morphogenesis in tumors. Circulating TEMs express low-level TIE2 (a), but the receptor is upregulated upon their extravasation and exposure to ANG2 in the perivascular microenvironment (b). TEMs adhere to ANG2-expressing sprouting blood vessels (b) and promote vascular growth (c and d).

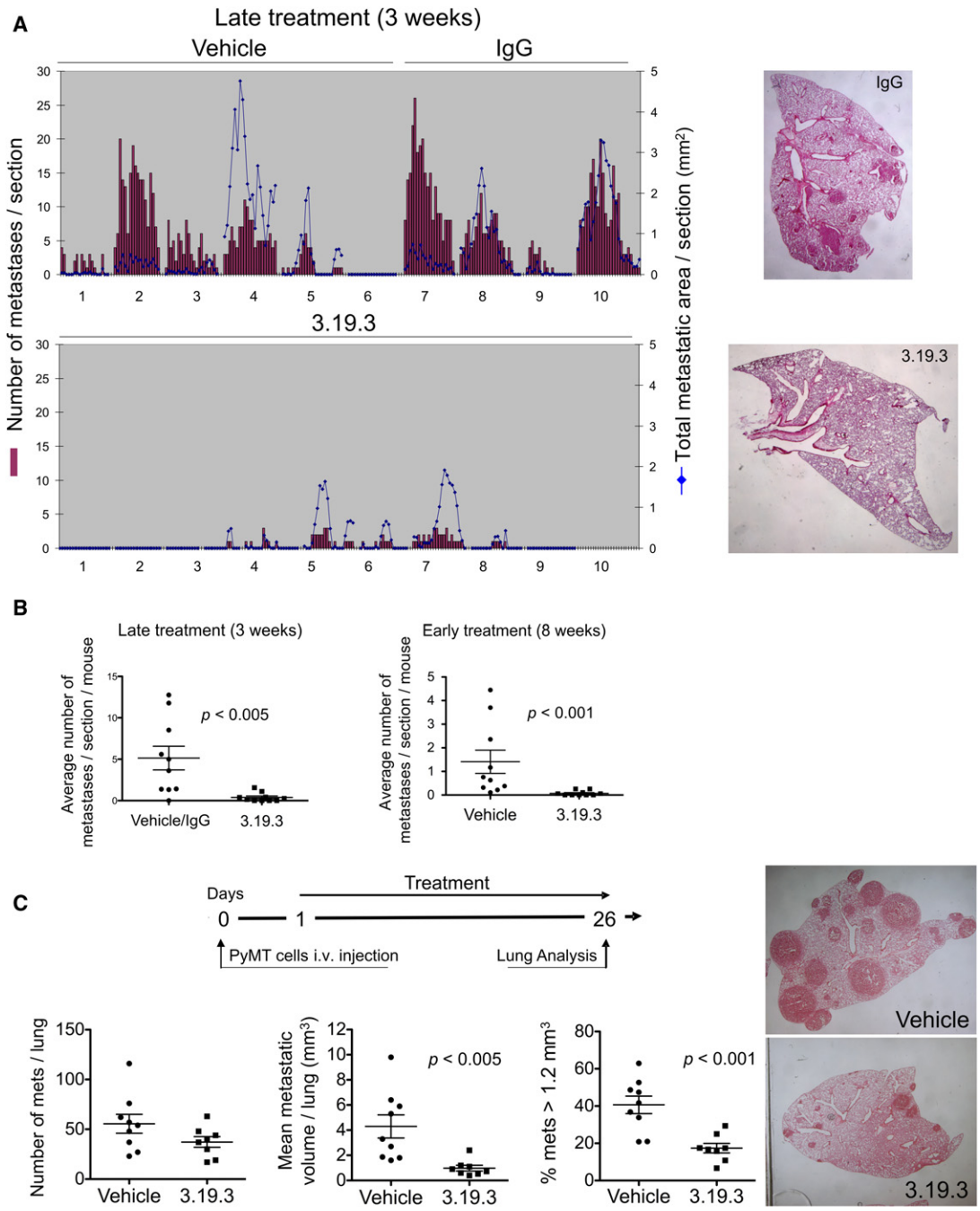

Figure 8. ANG2 Blockade Inhibits Spontaneous and Preestablished Mammary Tumor Metastasis

(A) Spontaneous metastasis model. Left panels illustrate number of metastatic foci (bars) and total metastatic area (broken line) in individual serial sections (each bar) obtained from the entire left lung of MMTV-PyMT mice treated with 3.19.3, control IgGs, or vehicle after a late schedule (see Figure 1A), and analyzed at 15 weeks of age. Right panels show H&E of representative whole lung sections.

(B) Spontaneous metastasis model. Number of metastatic foci (mean values ± SEM) per section per mouse in mice treated according to either late (3 weeks; left) or early (8 weeks, right; see Figure S8) schedules. Each dot represents one mouse. Statistical analyses by Mann-Whitney U test.

(C) Pre-established metastasis model. Top-left panel shows schematics of experimental design. Bottom-left panels illustrate morphometric analyses of metastasis (mean values ± SEM) in the lungs of mice either treated with 3.19.3 (n = 8) or vehicle alone (n = 9). Each dot in the plots represents one mouse. Results combine two independent experiments. Statistical analyses by Mann-Whitney U test (left and middle panels) or unpaired Student's t test (right panel). Right panels show H&E of representative whole lung sections.

subcutaneous tumors (Hashizume et al., 2010; Nasarre et al., 2009). Because ANG1 promotes pericyte-EC interactions, it is possible that ANG2 blockade by 3.19.3 increased ANG1 bioavailability for interaction with TIE2, thus enhancing pericyte coverage of the blood vessels and suppressing angiogenesis.

In agreement with previous findings (Fiedler et al., 2004), our gene expression data indicate that ANG2 is highly expressed in tumor ECs (Figure S4). However, the role of ANG2 in tumor angiogenesis is still controversial. L1-7N, a previously described ANG2-specific peptibody (Oliner et al., 2004), did not reduce vascular density detectably in the tumor models tested (Hashizume et al., 2010). Furthermore, genetic models of *Angpt2* deficiency or overexpression failed to unequivocally establish the importance of ANG2 in tumor angiogenesis (Chae et al., 2010; Nasarre et al., 2009).

Contrary to some of the earlier data, our findings indicate that 3.19.3 regresses the tumor vasculature and inhibits the growth of both early and late-stage tumors, pointing to a critical role of ANG2 during tumor progression. It is possible that some of the previously reported strategies of ANG2 inhibition might have overlooked the importance of ANG2 for tumor angiogenesis, particularly when both ANG2 and ANG1, which have opposite functions in tumor angiogenesis, were concomitantly targeted, e.g., by soluble TIE2 delivery or ANG1/ANG2-bispecific antibodies (Huang et al., 2010).

In MMTV-PyMT tumor models, 3.19.3 induced tumor blood vessel regression, increased tumor hypoxia, fibrosis, and necrosis, and enhanced the recruitment of MRC1$^+$ TAMs (i.e., TEMs) to the tumors. Such tumor responses were previously found—in the context of other antiangiogenic treatments (e.g., anti-VEGF/VEGFR) and/or tumor models—to associate with the activation of alternate proangiogenic pathways and drug resistance (Bergers and Hanahan, 2008; Casanovas et al., 2005; Shojaei et al., 2007). Accordingly, we observed increased expression of several proangiogenic genes (e.g., *Vegfa*, *Fgf2*, and *Sdf1*) in 3.19.3-treated mammary tumors. We currently ignore whether such upregulation of proangiogenic factors in 3.19.3-treated tumors is truly indicative of tumor adaptation to circumvent ANG2 blockade, rather than representing an epiphenomenon associated with enhanced tumor hypoxia or fibrosis. In either case we did not find evidence for drug resistance or rebound angiogenesis in tumors treated according to various ANG2 blockade schedules, pointing to a requisite role of ANG2 for tumor angiogenesis. Importantly, ANG2 blockade also inhibited angiogenesis and progression of late-stage, pancreatic insulinomas in RIP1-Tag2 mice, a mouse tumor model previously shown to develop resistance to anti-VEGF/VEGFR2 therapy (Casanovas et al., 2005; Shojaei et al., 2008). Although we did not directly compare ANG2 blockade with VEGF/VEGFR2 blockade, our data suggest that effective ANG2 inhibition may have the potential to achieve antiangiogenic and antitumor activity also in tumors that are resistant to anti-VEGF therapy.

Antimetastatic Activity of ANG2 Blockade

An important finding of this study is that ANG2 blockade markedly inhibited metastasis in two metastasis models. Clone 3.19.3 strongly inhibited spontaneous pulmonary metastases in MMTV-PyMT mice, both following short and extended (8 weeks) treatment schedules. These data argue that ANG2 blockade, at variance with certain models of anti-VEGF therapy (Ebos et al., 2009; Paez-Ribes et al., 2009), has potent antimetastatic activity and does not select for proinvasive/prometastatic tumor phenotypes. Because 3.19.3 reduced angiogenesis and increased pericyte coverage of the remaining blood vessels in the primary tumors, it is likely that tumor cell intravasation and dissemination were directly inhibited at the primary tumor site. Of note the genetic disruption of pericyte coverage elicited increased metastasis in the *Rip1*-Tag2 pancreatic islet tumor model (Xian et al., 2006).

Our data further indicate that 3.19.3 impairs the growth of micrometastases at the post-seeding step. Indeed, preestablished micrometastases failed to develop into large macrometastases following ANG2 blockade, a phenomenon possibly due to inhibition of the angiogenic switch that occurs at the metastatic site concomitant to micro- to macrometastasis transition.

The ANG2-TIE2 Pathway Regulates TEMs' Proangiogenic Activity

TIE2 is expressed at very low level in circulating monocytes but is strongly upregulated (up to 100-fold) in tumor-associated TEMs (De Palma et al., 2008). Thus, ANG2 may signal both autocrinally on ECs (Augustin et al., 2009) and iuxtacrinally on perivascular, TIE2$^+$ macrophages. The latter circumstance is supported by experimental evidence that ANG2 agonistically enhances the proangiogenic activity of human blood-derived TIE2$^+$, but not TIE2$^-$ monocytes in vitro (Coffelt et al., 2010b). Because the MRC1$^+$ TEMs recruited to 3.19.3-treated mammary tumors expressed much lower *Tie2* than those of untreated tumors, it can be envisioned that EC-derived ANG2 stimulates TIE2 expression on perivascular TEMs and that such feedback may be essential for the execution of productive angiogenesis. Although it cannot be excluded that TIE2 upregulation in TEMs is mediated indirectly by ANG2, ANG2 blockade specifically modulated the *Tie2* mRNA among several angiogenic genes analyzed, suggesting that this response is intimately linked to TIE2 signaling. Of note, several growth factors, including ANGs, can regulate the expression of their receptor tyrosine kinases at the transcriptional level via autoregulatory feedback loops (Hashimoto et al., 2004). Intriguingly, we did not observe transcriptional modulation of *Tie2* in ECs following ANG2 blockade; this may suggest that ANG2-mediated modulation of *Tie2* expression involves different TIE2 heterodimers (Seegar et al., 2010) and/or signaling adaptors (e.g., integrins) in ECs and TAMs.

To investigate the role of TIE2 in TEMs, we developed a gene knockdown platform that effectively protects the hematopoietic compartment from potential toxicity consequent to RNA interference in HSCs. Indeed, our previous attempts to knock down *Tie2* using constitutive LVs caused obvious hematopoietic toxicity (data not shown). By using inducible LVs coupled to detargeting from HSCs (Gentner et al., 2010), we showed that *Tie2* knockdown in BM-derived cells significantly inhibits angiogenesis and microvascular perfusion in MMTV-PyMT mice, without affecting hematopoiesis detectably. Remarkably, by targeting the TIE2 receptor in TEMs, we recapitulated some of the features of TEM elimination (De Palma et al., 2005), indicating that TIE2 is a pivotal biological effector and therapeutic target in these cells.

TAMs comprise molecularly and functionally distinct subpopulations (Qian and Pollard, 2010). TEMs express lower amounts of VEGF than classic TAMs (Pucci et al., 2009) and do not reside in hypoxic, avascular tumor areas (De Palma et al., 2005). Thus, it is likely that TEMs exert a requisite proangiogenic function by supporting tumor angiogenesis downstream to VEGF-induced vascular activation. Because the lower expression of *Tie2* in the TEMs of 3.19.3-treated mammary tumors was not associated with deregulated expression of a panel of classic pro- and antiangiogenic genes, one can envision that TIE2 expression by TEMs regulates blood vessel formation in tumors by noncanonical (e.g., VEGF-independent) angiogenic mechanisms. Indeed, our findings of impeded association between TEMs and tumor blood vessels both after specific *Tie2* knockdown in TEMs and extracellular blockade of ANG2 support the concept that the ANG2/TIE2 axis is crucial to establish cell-to-cell interactions between TEMs and ECs. Such scenario is in agreement with a recent study showing that $TIE2^+$ perivascular macrophages physically interact with the $TIE2^+$ endothelial tip cells of nascent blood vessels and are essential to promote vascular anastomosis during embryonic development (Fantin et al., 2010). Furthermore, $TIE2^+$ hematopoietic cells adhere to $TIE2^+$ ECs and stimulate angiogenesis in para-aortic splanchnopleural mesoderm explant cultures (Takakura et al., 1998). Both ANG1 and ANG2 induce homomeric TIE2 complex formation in cell-to-cell endothelial junctions (Saharinen et al., 2008). Thus, ANG2-mediated TEM-EC interactions may facilitate the navigation of endothelial sprouts through the dense extracellular matrix, eventually enabling the fusion of nascent blood vessels in angiogenic tissues (Figure 7I).

Tie2 silencing in TEMs, although consistently inhibited angiogenesis and tumor blood vessel perfusion by almost 50%, did not reproducibly inhibit tumor growth in the investigated mouse tumor models. Similarly, previous reports showed that the genetic deletion of certain proangiogenic factors in ECs or myeloid cells may reduce tumor angiogenesis without decreasing tumor growth rates (Nasarre et al., 2009; Stockmann et al., 2008). It should be noted that in our *Tie2*-silencing studies, from 10% to 50% of the tumor-associated TEMs were TIE2 competent (OFP^-) in the different mice. This is expected from the chimeric composition of hematopoiesis following transplantation of ex vivo-transduced HS/PCs and the nonexhaustive doxycycline-mediated gene induction. Thus, it cannot be excluded that fully exhaustive *Tie2* targeting in tumor-infiltrating macrophages would impair angiogenesis and tumor vessel function to an extent becoming critical for tumor growth.

In conclusion our data indicate that the TIE2 receptor expressed by perivascular TEMs is a crucial regulator of ANG2-mediated proangiogenic programs in tumors. Because tumor-infiltrating myeloid cells are known to convey protumoral and proangiogenic programs that can counteract the efficacy of antiangiogenic treatments (Bergers and Hanahan, 2008), the combined targeting of angiogenic ECs and proangiogenic TEMs by selective ANG2/TIE2-pathway inhibitors may extend the reach of antiangiogenic therapy in patients with cancer.

EXPERIMENTAL PROCEDURES

Detailed experimental procedures are available in Supplemental Experimental Procedures.

Mice

FVB and CD1 athymic mice were purchased from Charles River Laboratory (Calco, Milan, Italy). FVB/MMTV-PyMT and C57Bl/6/RIP1-Tag2 mice were obtained from the NCI-Frederick Mouse Repository (MD, USA) and established as colonies at the San Raffaele animal facility. FVB/*Pgk*-rtTA-miR-126T transgenic mice were generated by LV-mediated transgenesis. FVB/*Tie2*-GFP transgenic mice were generated previously (De Palma et al., 2005). All procedures were performed according to protocols approved by the Animal Care and Use Committee of the Fondazione San Raffaele del Monte Tabor (IACUC 324 and 335) and communicated to the Ministry of Health and local authorities according to the Italian Law.

ANG2 Blockade by 3.19.3

Tumor-bearing mice were randomized into vehicle (phosphate-buffered saline), IgG (Endobulin, Baxter, Italy), and treatment (3.19.3; AstraZeneca Pharmaceuticals, Waltham, MA, USA) groups. Clone 3.19.3 and IgGs were administered by i.p. injections after a twice-weekly schedule at doses of 10 mg/kg for the indicated periods of time, as described previously (Brown et al., 2010).

HS/PC Isolation, Transduction, and Transplantation for *Tie2* Knockdown in TEMs

BM was obtained from 6- to 12-week–old FVB/*PGK*-rtTA-miR-126T (LV2) transgenic mice. Lineage-negative cells enriched in HS/PCs were isolated using a cell purification kit (StemCell Technologies) and transduced by concentrated LVs. Briefly, 10^6 cells/ml were prestimulated for 4–6 hr in serum-free StemSpan medium (StemCell Technologies) containing a cocktail of cytokines (IL-3, SCF, TPO, and FLT-3L; all from PeproTech) and transduced with amiR-expressing LVs (LV1) with a dose equivalent to 10^8 LV transducing units/ml, for 12 hr in medium containing cytokines. After transduction, 10^6 cells were infused into the tail vein of lethally irradiated, 5.5-week–old, female FVB or FVB/MMTV-PyMT mice (radiation dose: 1150 cGy split in two doses).

Induction of *Tie2* Gene Knockdown by Doxycycline Administration

Starting at 4 weeks after HS/PC transplantation (i.e., 9.5 weeks of age), FVB or MMTV-PyMT mice were moved to doxycycline-containing food (Charles River) and received i.p. injections of doxycycline (0.5 mg/mouse) every third day, until the end of the experiments (12.5–13.5 weeks of age for FVB and 15 weeks of age for MMTV-PyMT mice).

Statistical Analysis

In all studies, values are expressed as mean ± standard error of the mean (SEM) or 95% confidence intervals (1.96 × SEM), as indicated. Statistical analyses were performed by unpaired Student's t test, or Mann-Whitney U test, as indicated. Differences were considered statistically significant at $p < 0.05$. Statistical methods are described in full in the Supplemental Experimental Procedures.

SUPPLEMENTAL INFORMATION

Supplemental Information includes Supplemental Experimental Procedures, eight figures, and two movies and can be found with this article online at doi:10.1016/j.ccr.2011.02.005.

ACKNOWLEDGMENTS

We thank Francesca Sanvito and Martina Rocchi for help with pathology; Cesare Covino (ALEMBIC) for help with tumor imaging; Lucia Sergi Sergi for vector production; Giulia Escobar for help with some experiments; and ChingChing Leow (MedImmune, Gaithersburg, MD, USA) for helpful discussions. This research was supported by grants from the European Research Council (Starting Grant 243128/TIE2+Monocytes to M.D.P.; Advanced Grant 249845/TARGETINGGENETHERAPY to L.N.), the Associazione Italiana per la Ricerca sul Cancro (IG-2007 to L.N. and IG-2010 to M.D.P.), AstraZeneca (to L.N. and M.D.P), Fondazione Guido Berlucchi (to M.D.P.), and the Italian Ministry of Health "Challenge in Oncology" (to L.N.). E.Z. was supported by a FIRC fellowship. None of the authors has a financial interest related to this work.

Received: July 19, 2010
Revised: December 1, 2010
Accepted: February 14, 2011
Published: April 11, 2011

REFERENCES

Amendola, M., Passerini, L., Pucci, F., Gentner, B., Bacchetta, R., and Naldini, L. (2009). Regulated and multiple miRNA and siRNA delivery into primary cells by a lentiviral platform. Mol. Ther. *17*, 1039–1052.

Arai, F., Hirao, A., Ohmura, M., Sato, H., Matsuoka, S., Takubo, K., Ito, K., Koh, G.Y., and Suda, T. (2004). Tie2/angiopoietin-1 signaling regulates hematopoietic stem cell quiescence in the bone marrow niche. Cell *118*, 149–161.

Augustin, H.G., Young Koh, G., Thurston, G., and Alitalo, K. (2009). Control of vascular morphogenesis and homeostasis through the angiopoietin-Tie system. Nat. Rev. Mol. Cell Biol. *10*, 165–177.

Bergers, G., and Hanahan, D. (2008). Modes of resistance to anti-angiogenic therapy. Nat. Rev. Cancer *8*, 592–603.

Brown, J.L., Cao, Z.A., Pinzon-Ortiz, M., Kendrew, J., Reimer, C., Wen, S., Zhou, J.Q., Tabrizi, M., Emery, S., McDermott, B., et al. (2010). A human monoclonal anti-ANG2 antibody leads to broad antitumor activity in combination with VEGF inhibitors and chemotherapy agents in preclinical models. Mol. Cancer Ther. *9*, 145–156.

Casanovas, O., Hicklin, D.J., Bergers, G., and Hanahan, D. (2005). Drug resistance by evasion of antiangiogenic targeting of VEGF signaling in late-stage pancreatic islet tumors. Cancer Cell *8*, 299–309.

Chae, S.S., Kamoun, W.S., Farrar, C.T., Kirkpatrick, N.D., Niemeyer, E., de Graaf, A.M., Sorensen, A.G., Munn, L.L., Jain, R.K., and Fukumura, D. (2010). Angiopoietin-2 interferes with anti-VEGFR-2-induced vessel normalization and survival benefit in mice bearing gliomas. Clin. Cancer Res. *16*, 3618–3627.

Chan, D.A., Kawahara, T.L., Sutphin, P.D., Chang, H.Y., Chi, J.T., and Giaccia, A.J. (2009). Tumor vasculature is regulated by PHD2-mediated angiogenesis and bone marrow-derived cell recruitment. Cancer Cell *15*, 527–538.

Chung, A.S., Lee, J., and Ferrara, N. (2010). Targeting the tumour vasculature: insights from physiological angiogenesis. Nat. Rev. Cancer *10*, 505–514.

Coffelt, S.B., Lewis, C.E., Naldini, L., Brown, J.M., Ferrara, N., and De Palma, M. (2010a). Elusive identities and overlapping phenotypes of proangiogenic myeloid cells in tumors. Am. J. Pathol. *176*, 1564–1576.

Coffelt, S.B., Tal, A.O., Scholz, A., De Palma, M., Patel, S., Urbich, C., Biswas, S.K., Murdoch, C., Plate, K.H., Reiss, Y., and Lewis, C.E. (2010b). Angiopoietin-2 regulates gene expression in TIE2-expressing monocytes and augments their inherent proangiogenic functions. Cancer Res. *70*, 5270–5280.

De Palma, M., Venneri, M.A., Roca, C., and Naldini, L. (2003). Targeting exogenous genes to tumor angiogenesis by transplantation of genetically modified hematopoietic stem cells. Nat. Med. *9*, 789–795.

De Palma, M., Venneri, M.A., Galli, R., Sergi Sergi, L., Politi, L.S., Sampaolesi, M., and Naldini, L. (2005). Tie2 identifies a hematopoietic lineage of proangiogenic monocytes required for tumor vessel formation and a mesenchymal population of pericyte progenitors. Cancer Cell *8*, 211–226.

De Palma, M., Mazzieri, R., Politi, L.S., Pucci, F., Zonari, E., Sitia, G., Mazzoleni, S., Moi, D., Venneri, M.A., Indraccolo, S., et al. (2008). Tumor-targeted interferon-alpha delivery by Tie2-expressing monocytes inhibits tumor growth and metastasis. Cancer Cell *14*, 299–311.

DeNardo, D.G., Barreto, J.B., Andreu, P., Vasquez, L., Tawfik, D., Kolhatkar, N., and Coussens, L.M. (2009). CD4(+) T cells regulate pulmonary metastasis of mammary carcinomas by enhancing protumor properties of macrophages. Cancer Cell *16*, 91–102.

Du, R., Lu, K.V., Petritsch, C., Liu, P., Ganss, R., Passegue, E., Song, H., Vandenberg, S., Johnson, R.S., Werb, Z., and Bergers, G. (2008). HIF1alpha induces the recruitment of bone marrow-derived vascular modulatory cells to regulate tumor angiogenesis and invasion. Cancer Cell *13*, 206–220.

Ebos, J.M., Lee, C.R., Cruz-Munoz, W., Bjarnason, G.A., Christensen, J.G., and Kerbel, R.S. (2009). Accelerated metastasis after short-term treatment with a potent inhibitor of tumor angiogenesis. Cancer Cell *15*, 232–239.

Fantin, A., Vieira, J.M., Gestri, G., Denti, L., Schwarz, Q., Prykhozhij, S., Peri, F., Wilson, S.W., and Ruhrberg, C. (2010). Tissue macrophages act as cellular chaperones for vascular anastomosis downstream of VEGF-mediated endothelial tip cell induction. Blood *116*, 829–840.

Fiedler, U., Scharpfenecker, M., Koidl, S., Hegen, A., Grunow, V., Schmidt, J.M., Kriz, W., Thurston, G., and Augustin, H.G. (2004). The Tie-2 ligand angiopoietin-2 is stored in and rapidly released upon stimulation from endothelial cell Weibel-Palade bodies. Blood *103*, 4150–4156.

Gentner, B., Visigalli, I., Hiramatsu, H., Lechman, E., Ungari, S., Giustacchini, A., Schira, G., Amendola, M., Quattrini, A., Martino, S., et al. (2010). Identification of hematopoietic stem cell-specific miRNAs enables gene therapy of globoid cell leukodystrophy. Sci. Transl. Med. *2*, 58ra84.

Hashimoto, T., Wu, Y., Boudreau, N., Li, J., Matsumoto, M., and Young, W. (2004). Regulation of tie2 expression by angiopoietin–potential feedback system. Endothelium *11*, 207–210.

Hashizume, H., Falcón, B.L., Kuroda, T., Baluk, P., Coxon, A., Yu, D., Bready, J.V., Oliner, J.D., and McDonald, D.M. (2010). Complementary actions of inhibitors of angiopoietin-2 and VEGF on tumor angiogenesis and growth. Cancer Res. *70*, 2213–2223.

Holash, J., Maisonpierre, P.C., Compton, D., Boland, P., Alexander, C.R., Zagzag, D., Yancopoulos, G.D., and Wiegand, S.J. (1999). Vessel cooption, regression, and growth in tumors mediated by angiopoietins and VEGF. Science *284*, 1994–1998.

Huang, H., Bhat, A., Woodnutt, G., and Lappe, R. (2010). Targeting the ANGPT-TIE2 pathway in malignancy. Nat. Rev. Cancer *10*, 575–585.

Kerbel, R.S. (2008). Tumor angiogenesis. N. Engl. J. Med. *358*, 2039–2049.

Kioi, M., Vogel, H., Schultz, G., Hoffman, R.M., Harsh, G.R., and Brown, J.M. (2010). Inhibition of vasculogenesis, but not angiogenesis, prevents the recurrence of glioblastoma after irradiation in mice. J. Clin. Invest. *120*, 694–705.

Kozin, S.V., Kamoun, W.S., Huang, Y., Dawson, M.R., Jain, R.K., and Duda, D.G. (2010). Recruitment of myeloid but not endothelial precursor cells facilitates tumor regrowth after local irradiation. Cancer Res. *70*, 5679–5685.

Lin, E.Y., Li, J.F., Gnatovskiy, L., Deng, Y., Zhu, L., Grzesik, D.A., Qian, H., Xue, X.N., and Pollard, J.W. (2006). Macrophages regulate the angiogenic switch in a mouse model of breast cancer. Cancer Res. *66*, 11238–11246.

Mantovani, A., and Sica, A. (2010). Macrophages, innate immunity and cancer: balance, tolerance, and diversity. Curr. Opin. Immunol. *22*, 231–237.

Murdoch, C., Tazzyman, S., Webster, S., and Lewis, C.E. (2007). Expression of Tie-2 by human monocytes and their responses to angiopoietin-2. J. Immunol. *178*, 7405–7411.

Nasarre, P., Thomas, M., Kruse, K., Helfrich, I., Wolter, V., Deppermann, C., Schadendorf, D., Thurston, G., Fiedler, U., and Augustin, H.G. (2009). Host-derived angiopoietin-2 affects early stages of tumor development and vessel maturation but is dispensable for later stages of tumor growth. Cancer Res. *69*, 1324–1333.

Oliner, J., Min, H., Leal, J., Yu, D., Rao, S., You, E., Tang, X., Kim, H., Meyer, S., Han, S.J., et al. (2004). Suppression of angiogenesis and tumor growth by selective inhibition of angiopoietin-2. Cancer Cell *6*, 507–516.

Paez-Ribes, M., Allen, E., Hudock, J., Takeda, T., Okuyama, H., Vinals, F., Inoue, M., Bergers, G., Hanahan, D., and Casanovas, O. (2009). Antiangiogenic therapy elicits malignant progression of tumors to increased local invasion and distant metastasis. Cancer Cell *15*, 220–231.

Pucci, F., Venneri, M.A., Biziato, D., Nonis, A., Moi, D., Sica, A., Di Serio, C., Naldini, L., and De Palma, M. (2009). A distinguishing gene signature shared by tumor-infiltrating Tie2-expressing monocytes, blood "resident" monocytes, and embryonic macrophages suggests common functions and developmental relationships. Blood *114*, 901–914.

Qian, B.Z., and Pollard, J.W. (2010). Macrophage diversity enhances tumor progression and metastasis. Cell *141*, 39–51.

Saharinen, P., Bry, M., and Alitalo, K. (2010). How do angiopoietins Tie in with vascular endothelial growth factors? Curr. Opin. Hematol. *17*, 198–205.

Saharinen, P., Eklund, L., Miettinen, J., Wirkkala, R., Anisimov, A., Winderlich, M., Nottebaum, A., Vestweber, D., Deutsch, U., Koh, G.Y., et al. (2008). Angiopoietins assemble distinct Tie2 signalling complexes in endothelial cell-cell and cell-matrix contacts. Nat. Cell Biol. *10*, 527–537.

Seegar, T.C., Eller, B., Tzvetkova-Robev, D., Kolev, M.V., Henderson, S.C., Nikolov, D.B., and Barton, W.A. (2010). Tie1-Tie2 interactions mediate functional differences between angiopoietin ligands. Mol. Cell *37*, 643–655.

Shojaei, F., Wu, X., Malik, A.K., Zhong, C., Baldwin, M.E., Schanz, S., Fuh, G., Gerber, H.P., and Ferrara, N. (2007). Tumor refractoriness to anti-VEGF treatment is mediated by CD11b+Gr1+ myeloid cells. Nat. Biotechnol. *25*, 911–920.

Shojaei, F., Singh, M., Thompson, J.D., and Ferrara, N. (2008). Role of Bv8 in neutrophil-dependent angiogenesis in a transgenic model of cancer progression. Proc. Natl. Acad. Sci. USA *105*, 2640–2645.

Shojaei, F., Lee, J.H., Simmons, B.H., Wong, A., Esparza, C.O., Plumlee, P.A., Feng, J., Stewart, A.E., Hu-Lowe, D.D., and Christensen, J.G. (2010). HGF/c-Met acts as an alternative angiogenic pathway in sunitinib-resistant tumors. Cancer Res. *70*, 10090–10100.

Stockmann, C., Doedens, A., Weidemann, A., Zhang, N., Takeda, N., Greenberg, J.I., Cheresh, D.A., and Johnson, R.S. (2008). Deletion of vascular endothelial growth factor in myeloid cells accelerates tumorigenesis. Nature *456*, 814–818.

Suri, C., Jones, P.F., Patan, S., Bartunkova, S., Maisonpierre, P.C., Davis, S., Sato, T.N., and Yancopoulos, G.D. (1996). Requisite role of angiopoietin-1, a ligand for the TIE2 receptor, during embryonic angiogenesis. Cell *87*, 1171–1180.

Takakura, N., Huang, X.L., Naruse, T., Hamaguchi, I., Dumont, D.J., Yancopoulos, G.D., and Suda, T. (1998). Critical role of the TIE2 endothelial cell receptor in the development of definitive hematopoiesis. Immunity *9*, 677–686.

Venneri, M.A., De Palma, M., Ponzoni, M., Pucci, F., Scielzo, C., Zonari, E., Mazzieri, R., Doglioni, C., and Naldini, L. (2007). Identification of proangiogenic TIE2-expressing monocytes (TEMs) in human peripheral blood and cancer. Blood *109*, 5276–5285.

Xian, X., Hakansson, J., Stahlberg, A., Lindblom, P., Betsholtz, C., Gerhardt, H., and Semb, H. (2006). Pericytes limit tumor cell metastasis. J. Clin. Invest. *116*, 642–651.